Coaxial to Microstrip Transition Modeling andCharacterization

Rita Dias Carreira

rita.carreira@tecnico.ulisboa.pt

Instituto Superior Técnico, Lisboa, Portugal

January 2021

Abstract

Experimental characterization is an important step in high frequency circuits design. For that, an electrical connection between the device under test and the measurement equipment will be required. This affects the measured results. To subtract the electrical connection influence from measured results and obtain the device under test data, several de-embedding techniques can be used.

This work defines, tests and models two commonly used connections to a transmission line: welded SMA connectors and test fixture with SMA connectors.

Transmission line types were studied and, after an in-depth analysis, the microstrip line was the one chosen to work with. Two PCBs with seven transmission lines, with the same length but different widths, were designed and simulated with the Advanced Design System (ADS) software. The seven lines had theoretical characteristic impedance close to 50 Ω. An experimental analyse of the characteristic impedances of these lines was performed to choose the most matched one. The first PCB had welded SMA connectors to its transmission line and the second PCB was placed on a test fixture for testing. The SMA connectors and the test fixture's SMA connectors were connected to a calibrated 2-port VNA. S-parameters were obtained with a frequency sweep ranging from 100MHz to 14GHz.

The obtained results from the VNA, had both transmission line and SMA connector/test fixture's SMA connectors included. The comparison between the theoretical results and the experimental results enabled the creation of a model for the SMA connector. Due to the poor quality of the ground planes, a model of the test fixture's SMA connectors could not be obtained.

Keywords: Transmission lines, microstrip, S-parameters, Calibration, VNA, SMA, test fixture

1. Introduction

There are many ways to test a PCB with mounted components. The main way is using the SMA connector to connect the PCB to the exterior. The second most used approach to test PCBs and its mounted components is the test fixtures. Several published works tried to describe SMA connector's effect on the measures [1] [2]. The problem of these works are the lack of consistency, that is to say, the description of a SMA connector in lumped elements is not the same in all these works. The same problem is present in the test fixtures. The test fixture used in this work does not have previous work associated, the present work is the first approach to the model of the test fixture "Argumen's" (now HMS) Universal Test Fixture. The objectives of this work are to develop models both for SMA connector and for test fixture and to justify the discrepancy of the results between theoretical, simulated and experimental data.

This paper is divided in 6 chapters, transmission line's theory, S-parameters theory, VNA's calibration, SMA's model development, test fixture's model development and conclusions/ future work.

2. Transmission Lines

Most used transmission lines are planar types which can be produced using low-cost printed circuit board materials and processes. Some of the multiconductor transmission lines have a solid dielectric substrate including one or two layers of metallization with the signal and ground currents running in separate conductors.

When the frequency of the signals is such that the losses in the line are no longer sustainable, a different type of line must be deemed.

Most common types of transmission lines are presented in Figure 1.

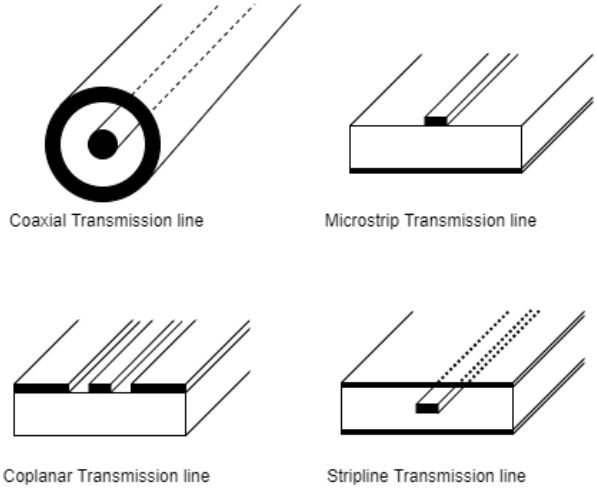

Figure 1: Typical transmission Lines [3].

A coaxial cable consists in two cylindrical conductors separated by a dielectric material which has a self shield property.

Stripline requires three layers of conductors: the internal (”hot” conductor), while the other two being the ”cold” or ”ground” conductor, consequently is also referred as tri-plate, as referred in [6].Stripline is close to a flexible and semi-rigid cable, it evolved from the coaxial cables. If pressure is applied to a coaxial cable, top and bottom, the circular structure starts to deform and goes to a elongated form. It maintained coaxial original sections but in a more operational form for higher frequencies and more efficient in Radio Frequency (RF)and microwave applications.

Microstrip line is a transmission-line geometry with a single conductor trace on one side of the dielectric substrate and a ground plane on the opposite side. In microstrip lines, small strips leads to higher losses and the thickness of the metal microstrip lines affect the insertion loss. Microstrip devices fabrication process creates some roughness, scratches and bumps on the metal surfaces to promote adhesion to the dielectric material. Electrical impact of conductor roughness increases with frequency, increasing the group delay and its capacitance as decreases the characteristic impedance over a wide bandwidth. Final plate impacts in the conductor loss due to high current density at the edge of the conductor. Most metal finishes used in Printed Circuit Board (PCB) fabric are less conductive than copper and a lower conductivity cause higher conductor losses, which increases insertion losses.

The alternative for stripline and microstrip transmission lines is the Coplanar Waveguide (CPW) which places both signal and ground currents on the same layer. The conductors form a center strip that is detached by a narrow gap from two ground planes on each side. The gap is usually very small and supports electric fields primarily concentrated in the dielectric.In order to concentrate the fields in the area for the substrate and minimize radiations, the substrate of the dielectric thickness is about twice the gap width.

The symmetrical structure in coplanar waveguides leads to a relative frequency independence of the effective permittivity that originates to a almost total lack of dispersion in the signal transmission, as portrayed in [4].

2.1. Attenuation in transmission lines

Attenuation in transmission lines can come from conductor losses (skin effect), dielectric losses and hysteresis losses, which are absorptive losses by nature and dissipate energy. Can also come from mismatch losses or even losses due to radiation which reflect and guide the energy away from the transmission line.

Skin effect attenuations are caused by the conducting medium series and can be described by following equation,

$$\delta[cm] = \frac{1}{2\pi}\sqrt{\frac{\rho}{f\mu_r}}, \tag{1}$$

where ρ is the specific resistivity of the conductor, μ_r is the conductor relative permeability - only considered when the material is ferromagnetic and as a relative permeability different from non-ferrous materials (this consideration were expressed in [5]).

Dielectric loss measures the electromagnetic energy dissipation. For an uniform filled transmission line the dielectric losses may be written as (2), as described in [6].

$$\alpha = 27.3\frac{\epsilon_r}{\sqrt{\epsilon_{eff}}}\frac{\epsilon_{eff}-1}{\epsilon_r-1}\frac{tan(\delta)}{\lambda_0}, \tag{2}$$

where tan(δ) is the loss tangent for the substrate material λ_g represents microstrip wavelength and is given by

$$\lambda_g = \frac{\lambda_0}{\sqrt{\epsilon_{eff}}}. \tag{3}$$

As the substrate thickness decreases, dielectric losses become more severe, reducing efficiency. On the other hand, when substrate thickness increases, the surface wave power also increases which limits efficiency.

When the magnetizing force (current) increase, the magnetic flux increases but when the magnetic force decrease, the magnetic flux does not decrease at the same rate. Therefore, flux density was still a positive value when the magnetic force reaches zero. One example of a theoretical curve

of losses for hysteresis is illustrated in Figure 2 and referenced in [4].

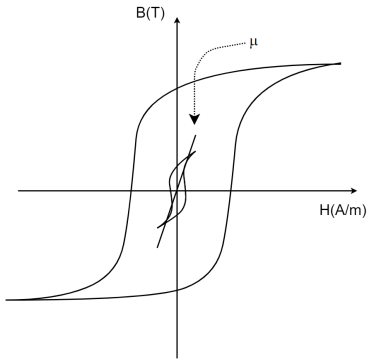

Figure 2: Hysteresis losses example [4]

In 2 the relation B-H is represented by and ellipse that results from hysteresis. The slope is the permeability of the material, μ. Ideally the ellipse that is represented in 2 must collapse into a line.

Mismatch losses occur when a discontinuity appears on a transmission line or when a termination of the transmission line is not equal to the characteristic impedance, as described in [5], therefore, in that location of the transmission line not all power is propagated, being reflected. Considering the transmission line and the load, not all energy is transferred to the load.

Discontinuities , like abrupt open-circuits, steps and bends will have losses due to radiation. Some of this losses cannot be eliminated to its full extension. Because radiation loss from an open ended waveguide can be extreme, they are usually short circuited at both ends forming a so called cavity. In high microwave frequencies, to reduce losses due to radiation, some cables are double and triple shielded. In addition, the passage of high frequency currents through an open wire increases electromagnetic field around it and the RF power is irradiated to free space or close circuits.

2.2. Comparison of transmission line types

Table 1: Comparison transmission lines

Transmission line	**Impedance range** $[\Omega]$	**Relative Dispersion**	**Relative circuit size**	**Relative Power handling capability**
Stripline	20-120	None	Large	Medium
Microstrip	20-120	Low	Small	High
Coplanar	40-110	Medium	Medium	Medium

In tables 2 and 3 are resumed advantages and disadvantages of the three referred transmission lines.

Table 2: Transmission lines' advantages

Transmission lines	Advantages
Stripline	The centered metal structure allows a good shield therefore there is a good isolation and lower attenuation loss. It has wider bandwidth.
Microstrip	Generally has rugged structures which handles higher voltage and power. It's compact size and light weight due to wavelength reduces to a third of its free space on account of the substrate fields.
CPW	Good for dense circuits due to crosstalk being limited by its geometry. CPW is not sensitive to substrate thickness and allows a wide range of impedance values on thick substrates. It resists discontinuities on the ground plane. Good for high frequencies.

Table 3: Transmission lines' disadvantages

Transmission lines	Disadvantages
Stripline	The structure is complex turning fabricating expensive and troubleshot hard.
Microstrip	Temperature variances must be accounted for because it limits the Average Power. Although being an advantage, small circuit dimensions might lead to problems in fabrication. The conductor losses increase with frequency. The quality factor is greatly reduced as thinner the substrate becomes.
CPW	Thicker substrates are needed therefore the size will be bigger and the fabrication more expensive. There is the possibility of transference of heat between close devices.

With the previous considerations and considering the present work goal, microstrip was the chosen transmission line for the current work.

3. S-parameters

In electronics, especially in microwave frequency range, it's hard to measure directly voltages and currents, it requires open or short connections and an ideal open isn't easy to create due to parasitic capacitance and radiation. In the case of shorts,the problem would be finite inductance.

Even so, necessity to describe networks is still present.

With that purpose, scattering matrix S were introduced in "S-Parameters Theory and Application" [7] in 1967 on HP Journal Cover, where it was called S-parameters.

In microwave frequencies, S-parameters are important considering they are easier than other parameters to measure and work at higher frequencies. Simpler, analytically convenient and direct, S-parameters are a measure of relative quantities.

S-parameters are reflection and transmission coefficients like gains or attenuations and are a way to describe n-port networks.

Like transmission lines, equations for S-parameters were obtained with derivatives off Maxwell equations. Maxwell equations were not used because it is not always possible or convenient to use these equations directly, solving them can be quite difficult and time consuming.

Considering that two networks are connected, once parameters in one network are measured, it's easier to predict their behavior on other network and characterize RF and microwave components that must operate together, including amplifiers and transmission lines or even free space.

Figure 3 is a network with 2-port,

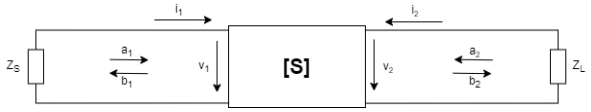

Figure 3: Two-port S-parameter network

where a_1 and a_2 are independent and normalized incident voltages while b_1 and b_2 are dependent and normalized reflected voltages, as follows:

$$a_1 = \frac{V_1 + I_1 Z_0}{2\sqrt{Z_0}}, \tag{4}$$

$$a_2 = \frac{V_2 + I_2 Z_0}{2\sqrt{Z_0}}, \tag{5}$$

$$b_1 = \frac{V_1 - I_1 Z_0}{2\sqrt{Z_0}}, \tag{6}$$

$$b_2 = \frac{V_2 - I_2 Z_0}{2\sqrt{Z_0}}. \tag{7}$$

Z_0 in the previews equations is the material's characteristic impedance.

S-parameters S_{11}, S_{12}, S_{21} and S_{22} can be described with help of a_1, a_2, b_1 and b_2, as follows:

$$S_{11} = \frac{b_1}{a_1} \tag{8}$$

, when $a_2 = 0$

$$S_{22} = \frac{b_2}{a_2}\Big| \tag{9}$$

, when $a_1 = 0$

$$S_{21} = \frac{b_2}{a_1}\Big| \tag{10}$$

, when $a_2 = 0$

$$S_{12} = \frac{b_1}{a_2}\Big| \tag{11}$$

, when $a_1 = 0$.

Each parameters has its own significance.

S_{11} is the input reflection coefficient with output port terminated by a matched load, S_{22} is the output reflection coefficient with input terminated by a matched load, S_{21} is the forward insertion (transmission) gain with output port terminated in

a matched load and the S_{12} is the reverse insertion (transmission) gain with input port terminated in a matched load. In other words, S_{11} and S_{22} are the optical reflection coefficients, S_{12} and S_{21} are the optical transmission coefficients.

As is known, input impedance at port 1 is measured with: he following equation.

$$Z_1 = \frac{V_1}{I_1} \tag{12}$$

It's to be noticed that

$$S_{11} = \frac{\frac{V_1}{I_1} - Z_0}{\frac{V_1}{I_1} + Z_0} = \frac{Z_1 - Z_0}{Z_1 + Z_0} \tag{13}$$

Considering a two-port network, S can be written as a 2x2 matrix:

$$\begin{bmatrix} b_1 \\ b_2 \end{bmatrix} = \begin{bmatrix} S_{11}S_{12} \\ S_{21}S_{22} \end{bmatrix} \begin{bmatrix} a_1 \\ a_2 \end{bmatrix}$$

The linear equations that describes two-port equations are:

$$b_1 = S_{11}a_1 + S_{12}a_2, \tag{14}$$

$$b_2 = S_{21}a_1 + S_{22}a_2. \tag{15}$$

This relations are the basis of the Smitch Chart transmission line calculations.

4. Calibration

one of the fundamental concepts in high-frequency is the know-how of waves travelling in a transmission line. In network analysis, this concept is transformed into the study of the ratios between reflected and transmitted signals on the DUT. Components are tested for several reasons,the main of them is to verify simulation models and proper functioning of hardware - compulsory when selling to a consumer and need to prove proper behavior. For these tests, a VNA is used. VNA is a test instrument that measures the response of a network as a vector, it acquires real and imaginary parameters and evaluates performance of the network. For this reason this device is a vital item of the RF design laboratories as in many manufacturing areas.

In order to measure incident, reflected and transmitted signals there are four sections in the network analyzer as referred next and on Figure 4:

1. Source of stimulus;
2. Signal separation devices;
3. Receivers that detect the signals;
4. Processor/ display for calculation and reviewing results.

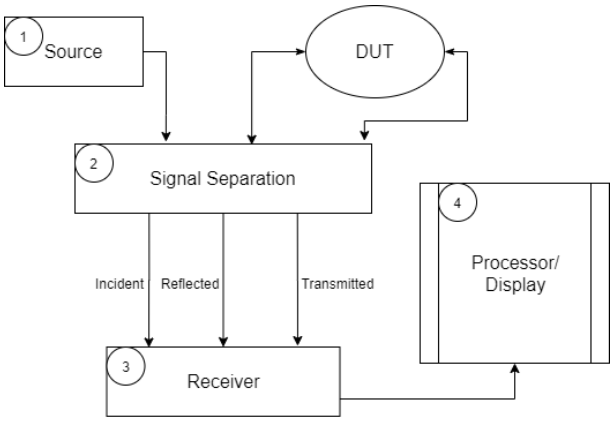

Figure 4: The 4 blocks - Network Analyzer

The first block is the signal source which gives stimulus to the system.

The second block is the signal separation device and has two functions. The first function is the measurement of a sample of the incident signal - done with splitters or directional couplers. Splitters are non-directional devices. Directional couplers[1] have low insertion loss, good isolation and directivity. The second function is the separation of forward and reverse waves at the output of the DUT.

The third block is the receiver block. There are two ways to detect a signal in network analyzers: Diode detectors and tuned receivers. The diode detector block converts the RF signal level to the correspondent DC level. The use of the diode allows the analysis of a range of frequency ($>$10 MHz to $<$26.5 GHz), its use is less expensive compared with using a tuned receiver. The diodes are also capable of measuring signals below -60 dBm and have a dynamic range around 60-75 dB. The problem about the diode is its frequency coverage limitation of sensitivity, making them susceptible to source harmonics and artificial signals. Tuned receivers use a local oscillator to mix RF into an intermediate frequency. Tuned receivers have better sensitivity and dynamic range, and contrary to diodes, reject harmonic and artificial signals - this comes from the narrowband of the tuned receivers. Furthermore, the dynamic range is improved when increasing power and, as mentioned before, decreasing frequency.

The fourth block of the network analyzer is the processor/display. In this block lays the process of changing and displaying information to the user in a more readable and easy way. Results can be presented in linear/logarithmic sweeps and formats like Smith charts, polar plots, etc.

[1] Considering the difficulty to make true broadband couplers, it is common to install bridges instead. Even though bridges have more losses and are unable to work in DC (the operation is similar to the Wheatstone bridge but with a unbalanced bridge - measuring both magnitude and phase through the bridge one can deduct the complex characteristic impedance).

In network analyzers three types of errors can occur: systematic, random and drift.

The systematic errors are due to a faulty equipment or bad experiment design. They are usually derived from incorrect calibration or improper use. They are predictable and removed mathematically during measurements.

Two major systematic errors are directivity and crosstalk.

Crosstalk is an isolation error. Isolation errors arise from signals, other than the transmission signal, leaking to the test receiver. Directivity is the main reason why a large ripple pattern is seen in several measurements of return losses. In their ripple peaks, directivity is adding in phase with reflection from the DUT. Adding to isolation and directivity errors, there are also source and load match errors. The source match error comes from the reflection signal of the DUT. It is reflected at the signal source and goes back to the DUT. The load match error is equivalent to the source match error. The error appears when a part of the transmitted signal is reflected at the response port and the measured signal is not the total of the sent signal. The last two systematic errors are called reflection and transmission tracking error and are related to frequency. The reflection tracking error is caused by differences in frequency response between incident and reflected signal at the receiver. The transmission tracking error is caused by the difference in frequency response between the incident and the transmitted signal at the receiver.

Altogether there are 6 sources of systematic errors. When observed in the opposite signal direction, one can gather the 12 sources of systematic errors. These errors will be applied in the 12-Term Error Correction calculations.

Random errors (also called unsystematic) do not have a pattern, therefore they are unpredictable and cannot be removed by calibration. Usually this type of errors come from instrument noise.

Drift errors are caused by deviations in the performance of the instrument after calibration. Usually these types of errors come from temperature - expansion of connecting cables, etc. These errors can be removed with frequent calibrations whilst measuring.

There are two types of error correction - response error correction and vector error correction.

In response error correction a reference trace is stored in memory and is divided by its measurement traces. It is simple to perform, but only effective in some of the errors pointed before - the tracking ones.

In vector error correction it is required an analyzer that can measure magnitude and phase. Measurements are more accurate and the majority of errors can be disclosed. These errors can vary from simple vector normalization to a 12-term error correction.

Vector error correction allows the characterization of the systematic error terms. This process is performed by measuring known standards, calculating and storing the errors in the analyzer's memory and removing them from the next measurements.

There are two main vector error corrections, one-port and two-port calibrations.

One-port calibration only works with reflection and can remove three systematic errors - directivity, source match and reflection tracking.

The used technique for these three errors is 3-Term Error Model represented next on the diagram of signal flow 5.

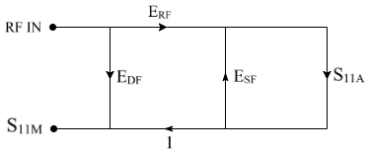

Figure 5: 3-Term Error Model [8]

In Figure 5, E_{DF} is the directivity error, E_{SF} is the port match error and E_{RF} is the tracking error. With 3-Term Error Model the relation between actual and measured reflection coefficients can be obtained.

Theoretical equations gives S_{11M} (S_{11} measured) and S_{11A} (S_{11} de-embedded) as follows,

$$S_{11M} = E_{DF} + \frac{S_{11A}(E_{RF})}{1 - E_{SF}S_{11A}}. \tag{16}$$

$$S_{11A} = \frac{S_{11M} - E_{DF}}{(S_{11M} - E_{DF})E_{SF} + E_{RF}} \tag{17}$$

Errors enforced in the previous equations are obtained by measuring the system using three independent standards where S_{11A} is known in all tested frequencies.

First standard is achieved when a "perfect load" is applied (hard to get by its own, good broadband is usually available in calibration kits to help achieve this), which makes S_{11A} = 0. Directivity is measured and E_{DF} is derived from equation 16. Only if S_{11A} is perfect can E_{DF} be measured directly. If it is not the case, it is a system of 3 equations for three unknown parameters.

As referred, there is no perfect load so there is always reflection, therefore any reflection from termination represents an error called match error.

An open circuit is enforced to establish the final standard. It is called tracking error.

Thus the values of the three errors, E_{DF} (directivity), E_{SF} (source match) and E_{RF} (reflection frequency response) are known and stored.

The diagram of signal flow of the 12-Term Error Model is represented on 6.

Figure 6: Forward 12-Term Error Model [9]

In Figure 6, E_{DF} is the directivity error, E_{SF} is the source match error, E_{RF} is the reflection tracking error, E_{TF} is the transmission tracking error, E_{LF} is the load match error and E_{XF} is the isolation error. These error are obtained from the forward diagram of the 12-Term Error Model signal flow.

With the same type of analysis done for one-port calibration (solving the flow graph) it is possble to achieve equations for S_{11A} and S_{21A}.

The missing six error coefficients are gathered in the reverse flow graph.

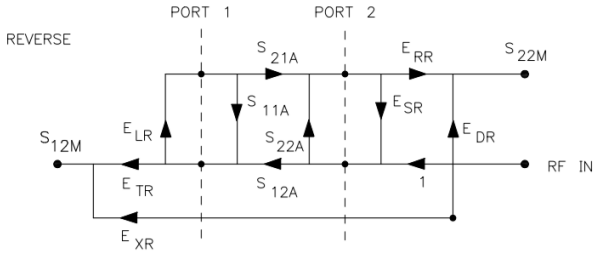

Figure 7: Reverse 12-Term Error Model [9]

In Figure 7, E_{DR} is the directivity error, E_{LR} is the source match error, E_{RR} is the reflection tracking error, E_{TR} is the transmission tracking error, E_{SR} is the load match error and E_{XR} is the isolation error. These error are obtained from the reverse diagram of the 12-Term Error Model signal flow.

Similarly to the previous two equations, S_{21A} and S_{22A} can also be deduced.

There are three steps that must be followed to obtain the unknown parameters presented in equations of S_{11A}, S_{12A}, S_{21A} and S_{22A}. The first step is coincident to one-port calibration. This step determines the directivity, the match error and the reflection tracking error. In step two, leakage and the crosstalk error are obtained from both ports by placing loads on each. In the last step, ports are connected. Port-2 match is measured directly with the calibrated port-1 reflectometer. With the two ports connected, the transmitted signal is derived and the transmission tracking is determined. These methods are applied in both forward and reverse models.

5. Results & discussion

In the development of this work, two experiments were performed. One based on ADS, a software from Keysight, and the other on the developed PCB. This PCB was tested on a VNA.

The first step of these experiments was the development of a PCB with seven lines with different widths, in ADS. These lines had characteristic impedances close to 50Ω. These width variations were made to evaluate the characteristic impedance variations between the lines. Considering the aspects mentioned in chapter 2, microstrip was the chosen transmission line to develop the PCB.

5.1. Prototype design

In the next figures are presented the schematic and the respective testbench of a simple microstrip line.

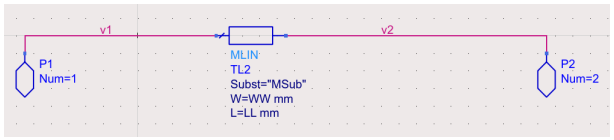

(a) Microstrip schematic

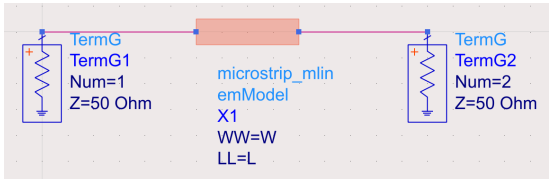

(b) Microstrip testbench

Figure 8: Schematic and testbench of microstrip line

The characteristics of the substrate used in the microstrip line are presented in the table 4.

Table 4: Characteristics of the substrate

Characteristic	Value
Substrate thickness (H)	1 mm
Relative dielectric constant (E_r)	4.37
Relative permeability (Mur)	1
Conductor conductivity (Cond)	5.7E+7
Cover height (Hu)	1.0e+33 mm
Conductor thickness (T)	35 μm
Dielectric loss tangent (TanD)	0.018
Conductor surface roughness (Rough)	0 mm

The line was implemented in a PCB with 7 different widths. The length of the lines is the same.

The values of the characteristic impedances, the attenuation and the delay of the line obtained with ADS are displayed in the tables 5 and 6.

Table 5: Characteristics (1)

Width (mm)	Impedance (real) Ω	Impedance (imag)Ω
1.28	61.42	0.39
1.58	54.89	0.36
1.78	51.30	0.34
1.88	49.69	0.33
1.98	48.18	0.32
2.18	45.44	0.30
2.48	41.89	0.28

Table 6: Characteristics (2)

Width (mm)	Attenuation (dB/cm)	Delay (ns/cm)
1.28	0.0635	0.0599
1.58	0.0640	0.0605
1.78	0.0643	0.0608
1.88	0.0644	0.06102
1.98	0.0646	0.0611
2.18	0.0650	0.0615
2.48	0.0653	0.0618

Considering the optimum case (the optimum case is an utopia, it is impossible to achieve in a real context), S-parameters are equal when considering S_{11} and S_{22}, and considering S_{12} and S_{21}.

In Figure 9, S_{11} and S_{22} are represented in blue and S_{12} and S_{21} are represented in red (as referred before, S_{11} and S_{22}, and S_{12} and S_{21} are coincident .

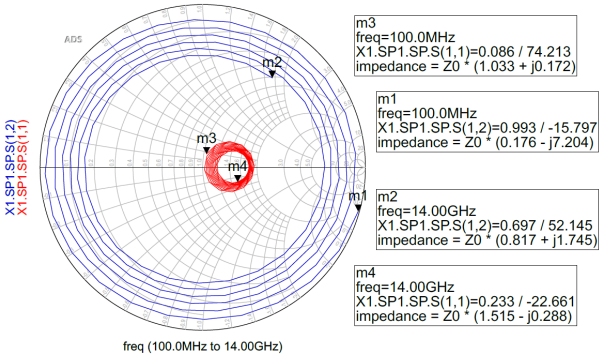

Figure 9: S-parameters S_{11} and S_{12} described with Smith Chart from ADS - line of 1.88mm of width

The layout of the PCB in ADS is presented in Figure 10.

Figure 10: Top View PCB

It is important to refer that the prints on the bottom view of the PCB are the same size of the ones on the top view.

As mentioned before, to test the PCB, connections to the exterior had to be made.

Several kinds of connectors are used to connect the exterior to the devices. Usually, the SMA connectors are used to connect coaxial lines and traces to the PCB.

The SMA connectors present good performance from DC up to 26,5GHz, as described in [10]. This component, when used with microstrip lines, offers excellent coupling characteristics and few undesirable properties.

The equivalent circuit model of the SMA connectors is represented in Figure 11 [11].

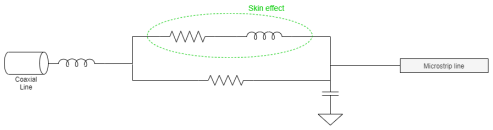

Figure 11: Circuit model of a coaxial connector

In this work, the true physical representation of the SMA connector was derived from the results of the modulations obtained.

5.2. Experimental results

The PCB was manufactured and used to perform tests of the SMA connectors to derive the SMA connectors' model and to test the miscrostrip lines' model accuracy.

Figures 12 and 13 were used to obtain the model of the SMA connector.

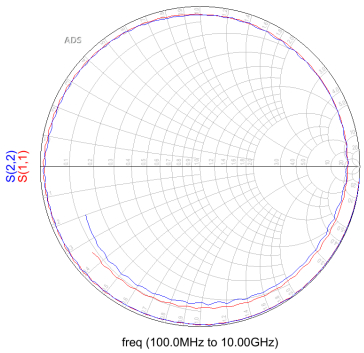

Figure 12: S_{11} and S_{22} representation in Smith Chart with open transmission line

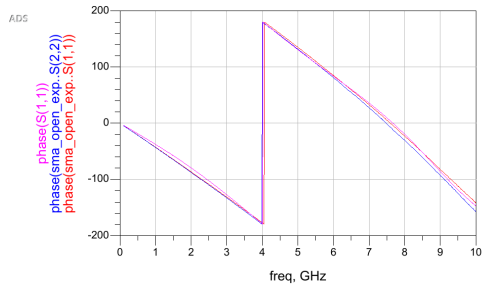

Figure 13: Phase graph used for tune - red and blue line refer to the experimental data, pink line refers to results of the SMA connector's model applied

Using a tuning tool included in ADS and the information presented in Figure 13 it was possible to obtain the SMA connector's model presented in Figure 14.

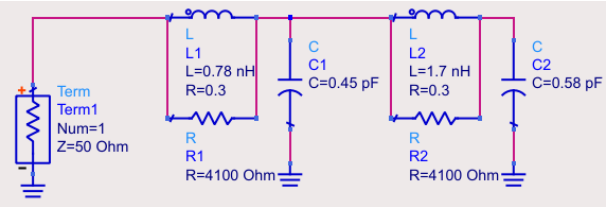

Figure 14: Complete SMA connector's model schematic with values

The results of this model are presented in Figure 15, where pink line represents the behaviour of a MLIN line in ADS with 1.88mm of width, blue and red lines are the applied model and black and green are the experimental results.

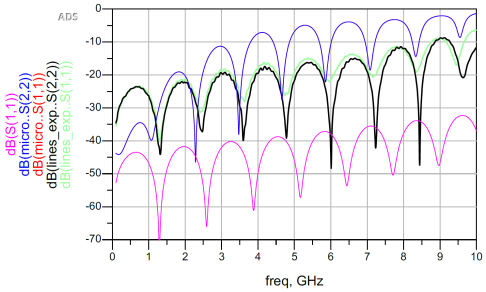

Figure 15: SMA model applied to MLIN of 1.88mm

It is visible from the previous picture that the model is not totally reliable. The minimums of the tests with the model of the SMA connector are not exactly in the same frequency as the experimental ones and neither are the values of magnitude. Nevertheless, it is a close model for the SMA connector considering that the behaviour of the simulated line follows the same behaviour as the experimental one.

Even with not so trustworthy results, the model of the SMA connector can be accepted to be a general model of this component, especially at lower frequencies.

5.3. Experiments with test fixture

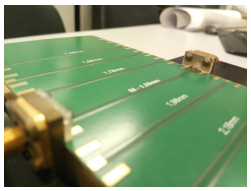

Figure 16: Test fixture detail

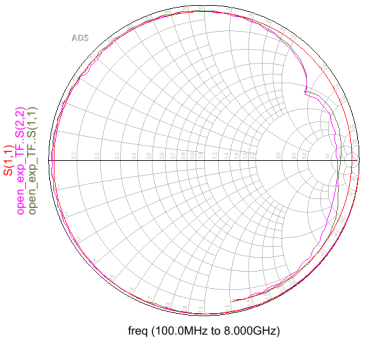

Figure 17: S_{11} and S_{22} representation in smith chart with an open transmission line on test fixture

In Figure 17 it is possible to notice a deviation of the line from what should be expected. This deviation can derive from the lack of ground existing in these connections.

In Figure 16, it can be seen that the connections between the PCB and the test fixture (on the upper side) only exist through mechanical pressure and there is no ground plane on the top.

The existence of a green layer on the PCB is also visible, it protects the metal from erosion. In the test fixture's case, this green layer was hampering the measures. On the backside ground plane, where the ground plane between the test fixture and the PCB should have been made, this green layer prevented the ground connectors from touching the ground plane of the test fixture, cutting its electrical contact. If a wave passes through the connector and the way back is blocked, or a path to return does not exist, the return of the wave becomes unknown and the correct results cannot be ensured.

These problems could be solved if a small quantity of weld was placed on the connectors on the backside of the PCB, in order to lift the ground plane.

With the previous considerations in mind, the model of the test fixture's SMA connector cannot be considered as a good model, nor can the values obtained be considered correct.

To obtain a proper test fixture's SMA connector model, an adequate ground plane must be as-

sured. The steps followed in this work, both for the experiment with the SMA connector and for the experiment with the test fixture, can be followed.

6. Conclusions

The goal of this work was the development of a SMA connector to microstrip transition model for welded and test fixture situations. In order to attain this objective, a PCB prototype was designed using the software ADS. This PCB included seven transmission lines as well as an open and a short line to be able to produce the models.

After manufacturing the PCB, its thickness was a concern. The PCB was fabricated with 1mm of thickness. This allowed the PCB to bend which could jeopardize the welds.

During PCB design the SMA connector dimensions for the PCB ground mask provided by the manufacturer were used. Later it was observed that there was not enough size for a reliable bottom ground plane welding. As a consequence this translated into incorrect results which were described throughout this work.

Even with some bad experimental results, it was still possible to obtain a model for the SMA connector to microstrip transition model for the welded case. The model is valid until 5GHz. For higher frequencies, the comparison between experimental and simulated results were significantly different. Developing a model for the test fixture was not possible. The obtained experimental data that was not reliable.

The test fixture's ground metallic parts touched the bottom of the PCB. The metal's protection layer of the PCB did not allow for a connection to be realized between the ground planes. Subsequently, collecting satisfactory results was not possible. Unfortunately there was no time, neither VNA availability, to repeat test fixture measurements after placing a superficial amount of solder in the bottom ground plate uncovered regions, that would allow a much better connection to ground.

This work's objectives also included the selection of the best line in terms of 50 Ohms characteristic impedance. It was concluded that 1.78mm was the most matched line considering its first four S_{11} magnitude lobes. These lobes were under -20dB which indicated lower mismatch. Its frequencies assumed values up to 5GHz. Exceeding this frequency value, mismatch is beyond acceptable.

Based on these conclusions, future studies should consider increasing the thickness of the PCB and enlarging the soldering area. When using the test fixture, the ground plane connection must be ensured.

Repeating this work with a more suitable ground plane is highly recommended in order to confirm if the results and conclusions presented can be applied on higher frequencies.

References

[1] J. Paleček, M. Vestenický, P. Vestenický, and J. Spalek. Examination of sma connector parameters. In *2012 IEEE 16th International Conference on Intelligent Engineering Systems (INES)*, pages 259–263, 2012.

[2] Takuichi Hirano, Jiro Hirokawa, and Makoto Ando. Influence of the sma connector and its modeling on electromagnetic simulation. *Microwave and Optical Technology Letters*, 57, 09 2015.

[3] Tullio Rozzi and Marco Farinai. Fundamentals of electromagnetics, 2011.

[4] Measuring Fluid Flow, Continuous Spinners, Full Bore, Flow Meters, Diverting Flow Meters, Log Format, Cable Speed, Sign Conventions, Fluid Flow Principles, Radioactive Tracer Tools, Oxygen Activation Logging, Oxygen Activation, Log Example, Schlumberger Water, Flow Log, Operating Principles, Stationary Oxygen, Activation Example, Stationary Oxygen, and Activation Example. Foundation For Microstrip Circuit Design, 2002.

[5] J. A. Bland and D. R. Bland. Wave Theory and Applications, 1991.

[6] Ramesh Garg; I J Bahl; Maurizio Bozzi. Microstrip lines and slotlines, 1996.

[7] Richard W. Anderson and Orthell T. Dennison. An Advanced New Network Analyzer for Sweep-Measuring Amplitude and Phase from 0.1 to 12.4 GHz. *Hewlett-Packard Journal*, (February 1967):2–9, 1967.

[8] A Complete Two-port Vector and Network Analyzer. A Complete Two-Port Vector Network Analyzer.

[9] Agilent Technologies and Network Analyzer. User ' s Guide. *Differences*, (April), 2012.

[10] Lighthorse Technologies. SMA Connectors, 2012.

[11] H. Zha, D. Lu, W. Wang, and F. Lin. Rf modeling and optimization of end-launch sma to trace transition. In *2015 IEEE 17th Electronics Packaging and Technology Conference (EPTC)*, pages 1–4, 2015.